Published in final edited form as:
J Neurogenet. 2012 March ; 26(1): 64–81. doi:10.3109/01677063.2011.652752.

Cyclic-AMP metabolism in synaptic growth, strength and precision: Neural and behavioral phenotype-specific counterbalancing effects between *dnc* PDE and *rut* AC mutations

Atsushi Ueda and **Chun-Fang Wu**
Department of Biology, University of Iowa, Iowa City, IA 52242, USA

Abstract

Two classic learning mutants in *Drosophila, rutabaga* (*rut*) and *dunce* (*dnc*), are defective in cAMP synthesis and degradation, respectively, exhibiting a variety of neuronal and behavioral defects. We ask how the opposing effects of these mutations on cAMP levels modify subsets of phenotypes, and whether any specific phenotypes could be ameliorated by biochemical counter balancing effects in *dnc rut* double mutants. Our study at larval neuromuscular junctions (NMJs) demonstrate that *dnc* mutations caused severe defects in nerve terminal morphology, characterized by unusually large synaptic boutons and aberrant innervation patterns. Interestingly, a counterbalancing effect led to rescue of the aberrant innervation patterns but the enlarged boutons in *dnc rut* double mutant remained as extreme as those in *dnc*. In contrast to *dnc*, *rut* mutations strongly affect synaptic transmission. Focal loose-patch recording data accumulated over 4 years suggest that synaptic currents in *rut* boutons were characterized by unusually large temporal dispersion and a seasonal variation in the amount of transmitter release, with diminished synaptic currents in summer months. Experiments with different rearing temperatures revealed that high temperature (29–30 °C) decreased synaptic transmission in *rut*, but did not alter *dnc* and WT. Importantly, the large temporal dispersion and abnormal temperature dependence of synaptic transmission, characteristic of *rut*, still persisted in *dnc rut* double mutants. To interpret these results in a proper perspective, we reviewed previously documented differential effects of *dnc* and *rut* mutations and their genetic interactions in double mutants on a variety of physiological and behavioral phenotypes. The cases of rescue in double mutants are associated with gradual developmental and maintenance processes whereas many behavioral and physiological manifestations on faster time scales could not be rescued. We discuss factors that could contribute to the effectiveness of counter balancing interactions between *dnc* and *rut* mutations for phenotypic rescue.

Keywords

cAMP; synaptic plasticity; excitability and fidelity

INTRODUCTION

Among the first learning and memory mutants isolated by forward genetic screening, *rutabaga* (*rut*; Duerr & Quinn, 1982) and *dunce* (*dnc*; Dudai et al., 1976) turned out to affect the enzymes that regulate cAMP metabolism. The *rut* gene encodes Ca^{2+}/calmodulin-

Corresponding Author: Dr. Atsushi Ueda, Dept. of Biology, University of Iowa, Iowa City, IA 52242, USA, Fax number 319-335-1103, Telephone number: 319-335-1090, atsushi-ueda@uiowa.edu.

activated adenylyl cyclase (AC; Levin et al., 1992) and *dnc* codes for cAMP specific phodphodiesterase (PDE; Chen et al., 1986), which are responsible for synthesis (Dudai et al., 1983; Dudai & Zvi, 1984; Livingstone et al., 1984) and degradation (Byers et al., 1981; Davis et al., 1981; Kauvar 1982) of cAMP, respectively.

Later studies have shown that altered cAMP levels in these mutants lead to not only memory deficiencies, but also a wide range of defects in neuronal development and function. In cultured neurons, *dnc* and *rut* displayed abnormalities in growth cone motility (Kim & Wu, 1996), neurite arborization (Peng et al., 2007), spike patterning (Zhao & Wu 1997), and Ca^{2+} signalling (Berke & Wu 2002). In larval neuromuscular preparations, altered phenotypes include alterations in motor terminal growth (Zhong et al., 1992; Zhong & Wu 2004), synaptic transmission (Zhong & Wu, 1991; Renger et al., 2000; Ueda & Wu, 2009), and ionic membrane currents (Zhong & Wu, 1993; Bhattacharya et al., 1999). In the adult CNS, modified habituation in an escape reflex circuit (Engel & Wu, 1996) and altered developmental processes of mushroom bodies (Technau 1984; Balling et al., 1987) have been implicated in the mechanisms of learning and memory deficiencies (Dudai et al., 1976; Tully & Quinn 1985; Gong et al., 1998; Gailey et al., 1984; Aceves-Pina et al., 1979).

Because of the opposing effects on cAMP levels by *dnc* and *rut*, one might expect that their phenotypes can be partially compensated and become milder in *dnc rut* double mutants. Such counterbalancing effects have been demonstrated between mutations with opposing effect on membrane excitability. For example, reduction in Na^+ channel expression caused by the nap^{ts} mutation effectively suppresses leg-shaking (*Sh*, *eag*, and *Hk*) and bang-sensitive (*bss*, *bas*, *eas*, and *knd*) hyperexcitability phenotypes through their counterbalancing effects on nerve membrane excitability (Ganetzky & Wu, 1982a, b; Budnik et al., 1990). Indeed, rescue of certain phenotypes in double mutants has been documented. For example, the increased numbers of terminal varicosities and branches in *dnc* larval neuromuscular junctions (NMJs) can be suppressed by *rut* in *dnc rut* double mutants (Zhong et. al., 1992) and the retarded growth cone motility of *dnc* and *rut* neurons in culture is partially restored in double mutants (Kim & Wu, 1996). On the other hand, many mutant phenotypes remain conspicuously abnormal in cultured neurons and in the adult giant fiber (GF) escape circuit in *dnc rut* double mutants. The erratic firing patterns of cultured neurons in *dnc rut* are as extreme as those in the corresponding single mutants (Zhao & Wu, 1997) and the altered habituation of adult GF escape circuit becomes even more extreme in *dnc rut* flies (Engel & Wu 1996). Similarly, the performance index for olfactory classical conditioning is further decreased in *dnc rut* compared to either single mutant (Tully & Quinn, 1985; Feany, 1990). However, there has been no report on the effects of combining *dnc* and *rut* on their physiological phenotypes in the larval preparation of the double mutants. This gap in the study of *dnc* and *rut* mutant phenotypes prompted us to examine previously unexplored interactions between *dnc* and *rut* at the larval NMJ. A wealth of background knowledge for development and function of this preparation allows a detailed investigation into cellular phenotypes exhibited in *dnc rut* double mutants. Here we report striking alterations in synaptic structure and transmission at the single-bouton level in *dnc* and *rut* mutants and describe phenotype-specific rescuing effects of combining *dnc* and *rut* mutations in double mutants.

MATERIALS AND METHODS

Drosophila Stocks

The *Drosophila melanogaster* stocks used include a wild-type (WT) strain Canton-S and mutant alleles of *rutabaga* (rut^1, rut^2, and rut^{1084}), *dunce* (dnc^1, dnc^{M11}, and dnc^{M14}), and *dnc rut* double mutant combinations (dnc^1 rut^1, dnc^{M14} rut^1). Use of independent isolates of mutant alleles helped exclude the possibility of phenotypic contributions from unidentified

second-site genetic variations. These lines have been previously described (Renger et al., 2000; Zhong et al., 1992; Kim & Wu, 1996; Peng et al., 2007). GAD-RFP is a generous gift from Dr. Paul Salvaterra.

Fly stocks were maintained at room temperature. However, the building room temperature varied significantly over the seasons between 1997 and 2001, as low as 15 °C during winter and as high as 30 °C during summer. Focal recording was carried out during this period. Intracellular excitatory junctional potential (ejp) recording was performed after 2002 when the building temperature was maintained at 22 to 24 °C throughout the year. To examine the effect of rearing temperature, we compared the stocks maintained at room temperature with those reared in 29–30 °C incubators (Fig. 5).

Larval Neuromuscular Preparations and Physiological Solutions

Post-feeding third instar larvae were dissected in Ca^{2+} free HL3 saline (Stewart et al., 1994) containing (in mM) 70 NaCl, 5 KCl, 20 $MgCl_2$, 10 $NaHCO_3$, 5 Trehalose, 115 Sucrose, and 5 HEPES, at pH 7.2. For physiological recordings, we used either HL3 (focal recording in Figs. 2, 3, 4, and 6) or HL3.1 (Feng et al., 2004), which have the same ionic conposition except for a reduced Mg^{2+} concentration (4mM, whole cell excitatory junctional potential recordings, Fig. 5). The final Ca^{2+} concentration in recording saline is specified for each experiment. To evoke nerve action potentials and ejcs, the segmental nerves were severed from the ventral ganglion and stimulated with a suction electrode (10 μm inner diameter) through the cut end. Stimulation amplitude was adjusted to 2.0 to 2.5 times the threshold voltage to ensure a uniform stimulation condition among experiments. Stimulus duration was 0.1 or 0.5 ms.

Focal Loose Patch-Clamp Recording

Extracellular focal recordings were performed as described previously (Renger et al., 2000; Ueda & Wu, 2009). Briefly, fire-polished focal recording electrodes with inner diameter of 4–8 μm and outer diameter of 15–20 um were filled with HL3 saline and were placed over type I boutons on muscle 13. The pipette opening typically covered one type Ib bouton. Ejc signals were picked up with a loose-patch clamp amplifier (Patch Clamp 8510; Zeitz Instruments, Munich, Germany) and stored on VCR tapes with a Pulse Code Modulator (Neuro Data, model Neuro-Corder DR-384, New York, NY). All trials contained a calibration pulse to determine the electrode series and seal resistance in order to correct for current leakage at the pipette tip (Renger et al., 2000; Kurdyak et al., 1994). In rare occasions, biphasic currents have been observed and they were excluded from data analysis.

Whole-cell excitatory junctional potential (ejp) recording

Nerve-evoked neurotransmitter release were also recorded intracellularly from postsynaptic muscle fibres 6 and 7 for experiments in Figures 5. Intracellular glass microelectrodes were filled with 3 M KCl and had a series resistance of about 60 MΩ. Ejps were picked up with a direct current pre-amplifier (model M701 micro-probe system, WPI, Conn., USA, and an additional custom-built amplifier).

Morphological examination of larval NMJs

To examine the morphology of NMJs, we performed immunostaining with anti-HRP antibodies and also employed the GAD-RFP line, in which red fluorescence protein (RFP) is expressed in motor neurons under the control of glutamic acid decarboxylase promotor (Featherstone et al., 2000). We crossed X^X; GAD-RFP with the X-linked *dnc*, *rut*, or *dnc rut* mutant and WT males, and the male progeny was examined. These approaches produced comparable results of NMJ morphology in WT and mutant larvae. To quantify bouton size,

anti-HRP staining images were collected with a high resolution lens to allow more precise measurements (for data shown in Fig. 1A, B). The FITC conjugated anti HRP antibodies were obtained from Jackson ImmunoResearch Laboratories (West Grove, PA, USA). The detailed protocol for anti-HRP staining of nerve terminals has been described previously (Lee et al., 2008).

Statistical Analysis

As described in the Results, ANOVA, student t-test, and Wilcoxon rank test with sequential Bonferroni adjustment for multiple comparisons were carried out.

RESULTS

Morphological alterations of nerve terminals caused by *dnc* and *rut* mutations

During the course of focal synaptic current recording under the Nomarski optics, we noticed striking alterations in bouton structures and motor terminal branch morphology not previously reported in *dnc* mutant larvae. We were prompted to analyze the morphology of individual boutons and axonal terminal projection patterns in *dnc* and *rut* single and double mutants in order to extend the previously described defects in gross branching pattern and bouton number (Zhong et al, 1992; Zhong & Wu, 2004). We focused our analysis on the identified motor terminals in muscle 13 of abdominal segments 3–5 to obtain uniform samples across different genotypes (dnc^{1}, dnc^{M11}, dnc^{M14}, rut^{1}, rut^{1084}, rut^{2}, dnc^{1} rut^{1}, dnc^{M14} rut^{1}).

In our morphological studies, we visualised motor terminals with anti-HRP staining and RFP expression in GAD-RFP larvae (see Methods). These two protocols produced consistent results and the data were pooled for the analysis of terminal projection pattern. The first notable abnormality in *dnc* terminal branches was a higher frequency of encountering unusually large boutons. Greatly increased bouton diameters were found in dnc^{M11} and dnc^{M14}, as measured by the largest bouton in each terminal branch (Fig. 1A, B. To quantify bouton size, anti-HRP staining images were collected with a high resolution lens to allow more precise measurements.). Some enlarged boutons were also found in *rut* although to a lesser degree of diameter increase (Fig. 1A, B). Another defect was that the motor axon often bifurcated before reaching the postsynaptic muscle, resulting in multiple, ectopic nerve entry points (Fig. 1C). Such defects in *dnc* were restricted to type Ib nerve terminals whereas their type Is terminals were morphologically indistinguishable from those in WT, indicating that *dnc* preferentially affects certain types of motor neurons. Our observation is consistent with the previous report of an increased higher order branches in *dnc* (Zhong et al., 1992, defects in type II terminals based on their small bouton size and branch locations).

We also observed another defect possibly derived from altered neuronal path finding in *dnc*, as indicated by abnormal projection patterns of Ib in relationship to Is motor terminals. In WT larvae, Ib motor terminals are closely associated with Is, running in parallel upon entering the target muscle (Fig. 1A). A similar case of close association of two types of motor terminal branches (tonic and phasic, homologous to type Ib and Is) has been described in crayfish muscles (Bradacs et al., 1997). We found that this pattern was not altered in *rut* larvae. However, in all three *dnc* alleles, the Ib terminal could run at a large angle away from the Is projection, resulting in a large separation between Ib and Is terminals. In more extreme cases, Ib branches entered the muscle cell at distant locations away from the Is terminal entry point (Fig. 1A). We quantified the degree of Ib-Is separation by measuring the distance from the tip of the Ib terminal to the Is branch (Ib is generally shorter than Is). The median distance for WT was 5 μm (25 ~ 75 % = 2.5 ~ 13 μm; the number of NMJs =

68) while that for *dnc* was 13 μm (25 ~ 75 % = 5 ~ 20 μm, N = 59, $p < 0.01$; rank-test with sequential Bonferoni correction). In contrast, the median for *rut* was 4.5 μm (25 ~ 75 % = 2.5 ~ 7.9 μm, N = 56) and was indistinguishable for that for WT ($p > 0.05$). These characteristic defects observed in *dnc* strongly suggest that abnormal levels of cAMP disrupt motor nerve terminal path finding and target interaction.

Counterbalancing effects of *dnc* and *rut* mutations on NMJ morphology

We asked whether any of the above developmental defects caused by defective cAMP degradation in *dnc* could be counterbalanced by disrupted cAMP synthesis caused by the *rut* mutation. Effects of their genetic interaction on specific phenotypes can be evaluated in *dnc rut* double mutants. The statistics presented in Figure 1 demonstrate that the ectopic multiple entry points of Ib terminal branches observed in *dnc* became less abundant in double mutants, consistent with a counterbalancing effect of *rut* (Fig 1AC). Furthermore, the separation between Ib and Is characteristic of *dnc* mutants became less striking as well in double mutants (The median of the distance between Ib tip to Is was 7.9 μm; 25 ~ 75 % was 5.0 ~ 10 μm; N = 38, $p > 0.05$ for the comparison with WT). However, not all of the above morphological defects could be rescued by combining *dnc* and *rut* in double mutants. The enlarged bouton size remained in double mutants, to an extent similar to that in *dnc* larvae (Fig. 1B).

These results suggest that the regulatory mechanisms of cAMP for motor axon path finding during terminal branch formation may be distinct from that for synaptic bouton differentiation or growth. It should be noted that in Figure 1B, only the size of the largest bouton in each terminal branch is presented, which displays considerable variability in *dnc* and in *dnc rut*. The overall bouton size distribution within individual terminal branches was also wide spread in *dnc* and remained so in *dnc rut* (data not shown). As a whole, altered cAMP degradation in *dnc* resulted in more severe modifications in synaptic bouton morphology and axonal terminal projection pattern than disrupted cAMP synthesis caused in *rut*, which lead to only mild defects (Fig. 1).

Focal recording of synaptic currents in *dnc* and *rut* neuromuscular junctions

Compared to morphological consequences, synaptic function at larval NMJs appeared to be more severely affected by *rut* than *dnc* mutations. We previously reported altered properties of synaptic transmission as characterized by focal patch recording in *dnc* and *rut* larvae (Renger et al., 2000; Ueda & Wu, 2009). In the present study, we employed patch electrodes of relatively large bores to monitor local activity of synaptic boutons along presynaptic terminal branches. This enabled us to detect activities in both Ib and Is terminals that ran in close parallel (see Methods and Renger et al., 2000; Ueda & Wu, 2009). Thus we were able to obtain a larger sample size of compound ejcs composed of contributions from both Ib and Is boutons in proximity. In a few experiments, we used pipets of smaller bores (less than 10 um outside and about 5 um inside diameter) to sample individual boutons along Ib or Is branches that ran separately. Notably, the conspicuously large, isolated Ib boutons in *dnc* were indeed functional but did not produce significantly lager focal ejcs than other Ib boutons of smaller sizes (data not shown).

For a given genotype, the compound focal ejcs can vary in amplitude to some extent along the same terminal branches but much greater variability can be observed among different branches or preparations (Ueda & Wu, 2009). Figure 2 presents ensembles of focal ejcs at a proximal site of the terminal branch on muscle 13 in abdominal segments 3 to 5 for each genotype. Data were collected under HL3 saline containing a physiological concentration of Ca^{2+} (1.5 mM). As previously shown, the most striking phenotypes in *rut* were decreased synaptic transmission (Fig. 2 AB) along with greatly increased temporal dispersion of

transmitter release (variation in time to peak, Fig. 2 CD). Another aspect of *rut* ejcs was the relatively high level of variability about the mean amplitude, as demonstrated by normalizing SD to mean ejc size (CV in Fig. 2F). Note that Figure. 2A shows representative superimposed traces of consecutive ejcs for each genotype and such data are rescaled and plotted sequentially in Figure. 2E to illustrate variability about the mean amplitude. By comparing properties of *dnc* and *rut* ejcs (Fig. 2), it is apparent that decreased cAMP levels caused by *rut* could lead to far more striking alterations in synaptic transmission than increased cAMP levels caused by *dnc*, consistent with the previous reports (Renger et al., 2000; Ueda & Wu 2009).

Synaptic transmission in *dnc rut* double mutants and variability in different genotypes derived from quantal fluctuation

We examined synaptic transmission in *dnc rut* double mutant larvae to reveal potential interactions of *dnc* and *rut* mutations. Interestingly, all aspects of *rut* defects described above were either restored to the WT level or considerably ameliorated. In double mutant larvae, ejc amplitudes became comparable to that in WT (Figs. 2AB); dispersion in transmitter release timing and fluctuation in release amplitude approached WT levels (Figs. 2C–F; similar results were observed in dnc^{M14} rut^{1} and dnc^{1} rut^{1}, and data from both genotypes were pooled). Presumably, the abnormal cAMP levels in *dnc* and *rut* presynaptic terminals was at least partially restored in double mutants (Livingston et al., 1984), rescuing a significant portion of defects in transmission properties. However, more detailed statistical analyses have provided some insights into the sources of the variability in transmitter release properties.

We examined how variability in the timing and amount of transmitter release could be correlated with ejc amplitudes in each mutant genotype as compared to WT. To analyse the ejc amplitude fluctuation across different amplitude ranges, we plot the CV of ejc amplitude for individual recording sites against mean amplitude in log-log scale (Fig. 3A). We found a progressive decrease in CV as mean amplitude increases in the WT sample, as predicted from the quantal nature of transmitter release, i.e. CV is proportional to sqrt (np(1-p))/np, or sqrt [(1-p)/np], where n is the number of releasing sites covered by the recording electrode and p is the probability of release per site and thus np is the mean quantal content for each ejc (Fatt & Katz, 1952; del Castillo & Katz, 1954). In our linear regression analysis, a predicted slope of 1/2 fits the data satisfactorily (Fig. 3A). Surprisingly, the *rut* data could be fit by the same regression line (Fig. 3A) despite the *rut* sample consisted a majority of small ejcs (Fig. 2B). Furthermore, ejc data from both *dnc* and *dnc rut* did not deviate substantially from the regression line fit to the WT data, despite their narrower amplitude ranges (Fig. 3A). Therefore the fluctuation in ejc amplitudes was governed by the statistics of the quantal nature of release, or vesicular exocytosis of transmitter, regardless of genotypes.

In a similar analysis, we plot SD of time to peak against log mean amplitudes for ejcs collected at individual recording sites (Fig. 3B). We found significant increase in temporal dispersion of ejcs in *rut* compared with WT ejcs across different amplitude ranges, as indicated by the substantially increased slope of the *rut* regression line than that of WT (Fig. 3B). Although ejcs of *dnc* and *dnc rut* were of larger amplitudes than those of *rut*, their SD of time to peak was still greater than WT for the respective amplitude range. Notably, the regression lines for these mutants lie above that for WT control (Fig. 3B).

Therefore, this extended statistical analysis enabled the detection of certain defects of *dnc* and *dnc rut* that are masked in Figure 2D. For example, the box plot shows increased spread of ejc timing only in *rut* but not in *dnc* or *dnc rut*. However, these comparisons are based on populations of different amplitude distributions; WT ejc amplitudes spanned a wider range whereas larger ejcs dominate in *dnc* and *dnc rut* data (Fig. 2AB). Thus, the extra

subpopulation of smaller ejcs (lower quantal contents) in WT, which are composed of fewer quanta, would in principle contribute to larger SD in time to peak (as compared to larger ejcs of greater number of quanta, which ensures more stable ejc peaking time). In fact, *dnc* and *dnc rut* ejcs produced greater SDs than WT ejcs of comparable sizes (Fig. 3B). These results indicate that altered cAMP metabolisms severely affects processes regulating vesicular release, causing dispersion in timing of transmission, which remains abnormal in double mutants. In contrast, the number of quanta released determines the magnitude of ejc amplitude fluctuations regardless of the cAMP levels in the various genotypes.

Temperature-dependent expression of *rut* phenotypes

The unusually large variability of ejc amplitudes in *rut* larvae lead us to a re-examination of the entire data set accumulated over a span of four years. We sought uncontrolled factors that were not obvious but might contribute to variation of the ejc size. Upon examination of daily records, we noticed that the smallest focal ejcs in *rut* tended to occur during summer times, but ejcs in other genotypes did not show clear seasonal effects (See combined monthly records in Fig. 4). Since the building temperature during the period of data collection was not strictly controlled (the room temperature fluctuated between 15 °C (winter) and 30 °C (summer), it suggests that temperature could have a major effect on *rut* phenotype expression.

We therefore examined the *rut* mutant phenotypes at different rearing temperatures. We exposed larvae to defined temperatures throughout their development (22–24 °C vs. 29–30 °C), and collected whole-cell ejps from matured 3rd instar laevae (wandering stage). We used HL3.1 saline with low Ca^{2+} (0.2 mM) to limit the amount of transmitter release and to increase the sensitivity to distinguish amounts of release with intracellular ejp recordings. Our results demonstrated that ejps in WT and *dnc* larvae remained unaltered at different rearing temperatures in amplitude and time course. Importantly, we found that rut^1 larvae reared at 22–24 °C produced ejps of nearly normal amplitude. In contrast, *rut* larvae raised at 29–30 °C showed clearly depressed synaptic release, as indicated by significantly smaller ejps, confirming the temperature-sensitive expression hypothesis (Fig. 5).

Significantly, the mutational effects of dnc^{M14} lead to increased ejp amplitudes at two different rearing temperatures, consistent with the previous report based on voltage-clamping measurements of whole-cell ejcs (Zhong & Wu, 1991). We first examined the effect of interactions between *dnc* and *rut* on ejp phenotypes at normal rearing temperature (22–24 °C). When dnc^{M14} was combined with rut^1, the ejp amplitude in double mutants was not distinguishable from WT measurements (Fig. 5). This apparent rescue effect was seen in the focal recording results (Fig. 2A), demonstrating a counterbalancing effect to restore enlarged *dnc* ejps to nearly normal amplitudes. However, when the rearing temperature was 29–30 °C, their interaction did not result in a clear rescue effect. The ejp amplitudes of dnc^{M14} rut^1 double mutants remained relatively small, closer to those of rut^1 than WT (Fig. 5). Thus, the rescue of *rut* defects at high temperature was less effective than at room temperature. In other words, the fundamental defects of transmission machineries in *rut* cannot be effectively reversed by cAMP level increases in dnc^{M14}. Presumably, the severely depressed transmission of rut^1 at 29–30 °C provided more stringent conditions to evaluate the rescuing effect of *dnc* and *rut* interactions.

It should be noted that ejp recording provides an indicator more relevant than focal ejc measurements to synaptic function at whole cell level. The failure of rescue of *rut* deficiencies in *dnc rut* ejps at high temperature (Fig. 5) was not reflected in our focal ejc recordings (Fig. 2AB). The focal recording was not carried out at strict temperature control and the data collection time periods did not significantly overlap among the three genotypes, dnc^{M14}, rut^1, and the double mutant dnc^{M14} rut^1 (see Fig. 4 and legends).

DISCUSSION

Differential effects of *dnc* and *rut* on synaptic terminal morphology and function

It has been demonstrated that cAMP levels are decreased in *rut* (Dudai et al., 1983; Dudai & Zvi 1984; Livingstone et al., 1984; Feany 1990) and increased in *dnc* (Byers et al., 1981; Davis & Kiger 1981). Our results clearly contrast the differential effects of disruptions in synthesis and degradation of cAMP on synaptic function and nerve terminal morphology. Mutations in *dnc*, including dnc^{1}, dnc^{M11}, and dnc^{M14}, can lead to severe defects in nerve terminal branching and bouton morphology (Fig. 1). Aside from this study, previous reports (Zhong e al. 1992, Schuster et al. 1996) have documented in identified larval muscles that total bouton numbers and motor terminal branching pattern are severely affected by *dnc*, but these defects were not detected in *rut*. A similar situation has been reported in the adult CNS: axon terminal growth in the mushroom body is enhanced in *dnc* but is not affected in *rut* (Peng et al. 2007). In contrast, *rut* and *dnc* mutations both have clear effects on synaptic transmission but in distinct manners. Increased cAMP levels in *dnc* could enhance transmitter release (as indicated by increased ejp sizes, Fig. 5) with a minimal disturbance in the temporal precision of the release process (SD of time to peak in focal ejcs, Figs. 2 & 3). In comparison, *rut* mutations more severely disrupt temporal control of release (Renger et al., 2000), regardless of the rearing temperature (Figs. 2 & 3). In addition, the rearing temperature affects the amplitude of synaptic transmission in *rut*, with strongly depressed transmission at high temperature (Figs. 2 & 3). This likely reflects a decrease in vesicle release because the miniature ejp size was unaltered at different temperatures (data not shown).

Comparisons of mutant alleles of *rut* and *dnc*

A number of mutant alleles of the *rut* gene have been described in the literature of developmental studies, but the alleles frequently used in neurogenetic experiments are limited to rut^{1}, rut^{2}, rut^{3}, rut^{1084}, and rut^{2080}. Furthermore, only three mutant alleles have been biochemically characterized in *Drosophila*, rut^{1}, rut^{2}, and rut^{3} (Dudai et al., 1983; Dudai & Zvi 1984; Livingstone et al., 1984; Feany 1990). It should be mentioned that these *rut* mutations can cause significant decrease in total cAMP synthesis despite the fact that there are at least 4 adenylyl cyclase (AC) homologous genes that have been identified molecularly and biochemically in *Drosophila* (Iourgenko et al., 1997; Iourgenko & Levin 2000; Cann & Levin 2000). This raises the possibility that *rut* may represent a major AC gene but all AC genes may play differential roles in regulating cAMP levels, depending on their subcellular localization and conditions to activate their actions. As demonstrated in this study (Fig. 6B for ejc amplitudes) as well as in earlier reports, a general pattern of relative severity among several *rut* mutant alleles is observed across different phenotypes, as represented in the following sequence: $rut^{1} >= rut^{1084} >= rut^{2} >= rut^{3} >=$ WT

Table 1 summarizes comparisons among *rut* alleles, which includes enzyme activity disruption (Dudai et al., 1983, Dudai & Zvi 1984; Livingstone et al., 1984; Feany 1990), suppression of high temperature- and hyperexcitability- induced NMJ growth (Zhong et al., 1992; Zhong & Wu 2004); suppression of increased neurite branching and GC size by high temperature or hyperexcitability (Peng et al., 2007); reduction of larval muscle Ca^{2+} current (Bhattacharya et al., 1999) and focal ejcs (Renger et al., 2000; this work), and deficiency in olfactory associative learning (Feany, 1990). It should be noted that the same sequence of severity is also observed among these alleles in rescuing egg development in the *dnc* mutant background (Bellen & Kiger, 1988).

Compared to the AC genes, there appears to be fewer PDE homologous genes and only two genes are known for their cAMP degradation action besides *dnc* (Day et al., 2005).

However, *dnc* gene products are represented by more than 10 splicing variants (Qiu et al., 1991; Davis & Davidson, 1986; as opposed to 2 *rut* splicing variants, Levin et al., 1992). There are a large number of *dnc* mutant alleles reported in literature but only a small number of them are frequently used in neurogenetic studies, i.e. dnc^{1}, dnc^{2}, dnc^{M11}, and dnc^{M14}. Interestingly, a consistent pattern of phenotypic severity can be observed across different phenotypes among these four alleles: $dnc^{M11} = dnc^{M14} >= dnc^{1} = dnc^{2}$.

A comparison of their effects on a variety of phenotypes is shown in Table 1, which includes PDE enzyme activity disruption (Davis & Kiger, 1981; Byers et al., 1981), defective growth cone motility of cultured neurons (Kim & Wu 1996), enhanced growth of larval NMJ (Zhong et al., 1992), enhanced K^+ (Zhong & Wu 1993) and Ca^{2+} (Bhattacharya ey al., 1999) current in larval muscles, decrease in the larval motorneuron firing frequency upon depolarization (Baines 2003), increase in whole cell ejps or ejcs (Zhong & Wu, 1991; This work) and decrease in activity-dependent facilitation of synaptic transmission (Zhong & Wu, 1991) at larval NMJ, decrease in the habituation rate of olfactory jump response (Asztalos et al., 2007) and odor-electric shock association (Dudai 1983; Tully & Gold 1993) in adult flies, and female sterility (Salz et al., 1982; Mohler & Carroll 1984). In a different approach, overexpression of a UAS-dnc^{+} transgene in motor neurons results in reduced NMJ growth and decreased ejp size even in larvae reared at RT (Cheung et al., 1999). These phenotypes demonstrated the effects of increased cAMP degradation in contrast to those caused by *dnc* mutations.

When considering their mechanisms of action, several reported phenotypic effects of *dnc* alleles may be complicated by the implications of contributions from the genetic background. Notably, the dnc^{M11} mutant line has been reported to affect protein kinase C (PKC) activity in addition to PDE (Devay et al., 1989). In addition, the severity of dnc^{1} may in fact be more extreme than reported (Fig. 1) since dnc^{1} has been shown to be female sterile once a second-site mutation near the *dnc* locus is removed from the original fertile line (Salz et al., 1982). It is possible that many dnc^{1} lines used in neurogenetic investigations contain this mutation in the background.

Comparisons of *rut* and *dnc* mutational effects across a variety of neural and behavioural phenotypes

A number of experimental paradigms have been used to characterize behavioural and physiological phenotypes of *dnc* and *rut* mutants with defined quantitative parameters. As summarized in Table 1, for a majority of phenotypes examined, *dnc* and *rut* mutations do not lead to opposite effects on these quantitative indices, even though they alter the cAMP levels in opposite directions. Only for certain phenotypes, the *dnc* and *rut* mutations affect the parameters in opposite directions. For example, in larval neuromuscular synaptic boutons, mobilization of synaptic vesicles from the reserve pool to exo/endo cycling pool is suppressed in *rut* and enhanced in *dnc* (Kuromi & Kidokoro, 2000). Similarly, the number of docked vesicles at synapses is decreased in *rut* and increased in *dnc* (Renger et al., 2000). Ca^{2+} current measured in larval muscles is decreased in *rut* and increased in *dnc* (Bhattacharya et al., 1999). Hyperexcitability-induced overgrowth of larval NMJ can be suppressed by *rut* but enhanced by *dnc* (Zhong et al., 1992). Similarly, *dnc* and *rut* mutations exert opposite effects on Kenyon cell axon counts in the mushroom body of developing adult flies (Balling et al., 1987). Finally, habituation rate of the giant fiber escape circuit is decreased by *rut* and increased by *dnc* (Engel & Wu 1996).

In contrast, for some other phenotypes, *rut* alleles have no apparent effects while *dnc* mutants display clear alterations (Table 1). For instance, the larval NMJ terminal projection pattern (Fig 1; Zhong et al., 1992) and adult mushroom body axonal terminal growth (Peng et al., 2007) were altered in *dnc* but not in *rut*. Moreover, identified K^+ currents (IA and IK)

in larval muscles are increased in *dnc* but unaltered in *rut* (Zhong & Wu, 1993). In these cases, increased cAMP levels can produce abnormalities but underlying mechanisms may be tolerant to depleted cAMP levels.

For another group of phenotypes, *dnc* and *rut* mutations can affect separate parameters and sometimes produce superficially similar effects by altering a parameter in the same direction (Table 1). Such cases include decreased growth cone motility (Kim & Wu, 1996), irregular action potential firing pattern (Zhao & Wu 1997), and modified intracellular Ca^{2+} dynamics (Berke & Wu 2002) in cultured neurons. In larval neuromuscular junctions, both *dnc* and *rut* decrease synchronicity of synaptic transmitter release (Renger et al., 2000) and presynaptic facilitation of neuromuscular transmission (Zhong & Wu 1991). During post-eclosion development of adult flies, both *dnc* and *rut* mutations enhance the axon terminal growth of mechanosensory cells (Corfas & Dudai, 1991) and decrease the structural and functional adaptation of the olfactory system to odor exposure (Devaud et al., 2001; 2003). Neither *dnc* nor *rut* mutants respond to environmental or social deprivation in modifying Kenyon cell axon counts of young adults (Balling et al., 1987). Mutations of either *dnc* or *rut* decreases habituation rate of the proboscis extension reflex and olfactory avoidance and jump response (Duerr & Quinn 1982; Asztalos et al., 2007; Das et al., 2011), and the performance indices of both classical (Folker 1982; Dudai 1983; Tully & Quinn 1985; Feany 1990; Gailey et al., 1984) and operant (Wustmann et al., 1998; Gong et al., 1998; Zars, et al., 2000; Liu et al., 2006; Brembs & Plendl 2008) conditioning. Studies on alcohol response have demonstrated increased sensitivity in *rut* alleles but no apparent change in *dnc* alleles (Moore et al., 1998). While it is reassuring to observe opposite effects of *dnc* and *rut* mutations on some of the quantitative parameters, it should be noted that it is not straightforward in associating most of the indicators with the defective mechanisms directly regulated by cAMP signalling. Dysfunction in AC and PDE may exert opposite effects on some cell biological mechanisms or neural circuit components but can still lead to apparently similar deficiencies of a cellular function or behavioural task (see last section of Discussion).

Counter-balancing interaction between *dnc* and *rut* mutations in double mutants: Nature of *rut* mutations

Some insights may be gained through examining the genetic interactions between *dnc* and *rut* in double mutants about how *rut* AC and *dnc* PDE are involved in particular aspects of physiological or behavioural plasticity. At the present time, only a limited number of reports document the resultant phenotypes in *dnc rut* double mutants (Table 1). Significantly, the majority of the single-mutant phenotypes of *dnc* or *rut* mutations do not become less severe in *dnc rut* double mutants, even though the overall cAMP levels are largely restored (Livingstone et al., 1984). The phenotypes that are not rescued in double mutants include increased bouton size in *dnc* (Fig. 1) and impaired synchronicity of transmitter release (Fig. 3) in larval NMJs, irregular firing of cultured neurons (Zhao & Wu, 1997), and habituation (Engel & Wu 1996) and olfactory associative learning (Tully & Quinn 1985; Feany 1990) of adult flies.

However, a few cases of successful rescue in double mutants have been described (Table 1). Decreased growth cone motility in *dnc* and *rut* neurons in culture can be restored by combining two mutations (Kim & Wu, 1996) and the overgrowth and altered projection patterns of *dnc* larval motor terminals is suppressed in *dnc rut* (Zhong et al., 1992; this study). Interestingly, none of the above cases of successful rescue involve opposite effects of *dnc* and *rut* single-mutant phenotypes (Table 1). Notably, both cases of restoration involve a particular allele, rut^1. The allele rut^1 is different from other alleles with characterized AC enzyme activity (rut^2 and rut^3) in that the Ca^{2+}/CaM-dependent activation of AC is eliminated in rut^1 flies (Dudai & Zvi 1984; Livingstone et al., 1984), but retained in rut^2 and rut^3 (Feany 1990). Unlike rut^1, the allele rut^2 is not able to rescue the *dnc* mutational effects

of enhanced larval NMJ growth (Zhong et al., 1992) and irregular firing in cultured neurons (Zhao & Wu, 1997). In our present study of NMJ focal recording, it was clears that *rut*^{2} did not affect the precision in release timing (ejc peak time) and ejc amplitudes, although *rut*^{1} decreased the temporal precision of release (increased variability in ejc peak time) and the ejc amplitude significantly (Fig. 6). It will be helpful if further experiments are performed on additional allele combinations of *dnc* and *rut* to delineate the role of Ca^{2+}-dependent regulation of AC in specific phenotypes of interest.

Conditions and factors that could restrict counterbalancing interactions of *dnc* and *rut*

In addition to peculiarities of enzymatic properties in mutant alleles, e.g., *rut*^{1} AC devoid of Ca^{2+}/calmodulin sensitivity, other factors influencing interactions between *dnc* and *rut* must be considered. As summarized above, counterbalancing rescue of *dnc* and *rut* phenotypes in double mutants is likely to be exceptions rather than a general rule. Therefore, it would be desirable to identify the conditions and factors that could facilitate their counterbalancing interactions, which may provide insights into the orchestration of *dnc* PDE and *rut* AC underlying the phenotype of interest.

First, it is important to consider the temporal and spatial characteristics of expression and operation of these enzymes. In the temporal domain, their effects on a variety of phenotypes are mediated through integration among different biochemical pathways and cellular processes, some of which may function with rapid kinetics, while others may represents slow accumulation of products through a number of steps. Some of the resultant phenotypes may require continuous adjustment in response to internal or environmental conditions while others may appear relatively permanent and irreversible, possibly associated with developmental events.

The spatial factors to be considered include the cellular expression and subcellular localization of the enzymes. To the best of our knowledge, there is little information about whether *dnc* PDE and *rut* AC are colocalized in molecular assemblies or aggregates within certain functional domains in specific neuronal cell types. Close proximity of AC and PDE localization facilitates local regulation of cAMP levels within a short time. Certain cellular processes with slower kinetic steps also facilitate integration of *dnc* and *rut* interactions, extending their balancing acts to a broader spatial range.

For the few examples of successful counter-balancing rescue, growth cone motility seems to be a continuous adjustment by cAMP on a time scale of tens of seconds to minutes (Song et al., 1997). This relatively slow kinetics make it possible to readily manipulate the cAMP signalling pathway, e.g., bath application of db-cAMP increases *rut* growth cones motility, mimicking *dnc* counter balancing effects in double-mutant growth cones (Kim & Wu 1996). Some developmental or maintenance processes, such as axonal path finding, branch formation, target interaction and synaptogenesis, are also slow adjustment processes (in the order of hours to days). In these cases, restoration of cAMP levels through long-range interactions of AC and PDE may be sufficient to rescue the single-mutant phenotype. For example, *dnc* defects in larval motor terminal growth are suppressed by *rut*^{1} (Zhong et al., 1992; this paper).

On the other hand, defects in some physiological properties (K^{+} currents, neuronal firing, and transmitter release timing) and behavioral conditioning (habituation and classical conditioning) can not be rescued by combining *dnc* and *rut*, which sometimes leads to even more extreme deficiencies, e.g., the extremely rapid habituation in *dnc rut* (Engel & Wu 1996). One possibility is the requirement of dynamic cAMP regulation within a short time period (milli-second to second range) during which a counter-balancing act is difficult to achieve. Another possible explanation is the requirement of unimpaired cellular machinery

laid down during development (e.g., proper channel and receptor localization) and functional connectivity among synaptic partners (inhibitory and excitatory elements in the circuit) underlying behavioural phenotypes under consideration. Deviation from coordinated actions of such subcellular machinery or circuit components will make it difficult to obtain compensatory rescue.

It should be noted that well-defined abnormalities in central fiber projection have been reported in *dnc* and *rut* single mutants (Corfas & Dudai 1991; Balling et al., 1987; Peng et al., 2007) that reflect the alterations in peripheral motor terminals in larval NMJs (Fig 1; Zhong et al., 1992). Furthermore, *dnc* PDE and *rut* AC are preferentially expressed in mushroom bodies, which are important in odor-associated learning (Nighorn et al., 1991; Han et al., 1992). Therefore it is reasonable to speculate that defects in higher functions, including classical associative learning and habituation, may involve anatomical defects in the CNS, such as altered dendritic arbors and synaptic connections detectable in certain defined circuits, in addition to potential changes in synaptic physiology (Engel & Wu, 1996).

Cell-specific expression and subcelular localization of AC and PDE isoforms may affect *dnc* and *rut* single-mutant, as well as double-mutant phenotypes. These include spiclicing variants of the *dnc* and *rut* gene as well as the products of their homologous genes. Such complexity needs to be considered in the interpretation of *dnc* and *rut* interactions in order to appreciate contributions of individual splicing variants and to delineate influence from their homologous genes.

Finally, cross talk between the cAMP and other signaling pathways can also modify *dnc* and *rut* phenotypes. For example, variety of signalling pathways are known to converge onto the CREB transcription factor (Johannessen & Moens 2007). It is also established that not only the cAMP cascade but also other signaling pathways, including PKG (Renger et al., 1999) and CaMKII (Griffith et al., 1994) can modify larval NMJ physiology and morphology as well as adult habituation (Engel et al., 2000; Engel & Wu 2009 for review), courtship conditioning (Griffith & Ejima 2009 for review) and classical conditioning (Davis 2005 for review; Mery et al., 2007). It will be of particular interest to establish the consequences of such genetic interactions across signaling pathways. Double mutant analysis in conjunction with transgenic and genomic approaches remains a powerful and profitable direction for revealing the genetic network underlying neural and behavioral plasticity.

Acknowledgments

This paper was written to commemorate Professor Yoshiki Hotta’s retirement. We thank Xuxuan Wan and Xiaomin Xing for their assistance in the NMJ morphological studies using GAD-RFP and anti-HRP staining techniques. We thank Atulya Iyengar for his comments on our manuscript. We also thank to Dr. Paul Salvaterra for his generous gift of the GAD-RFP line. This work was supported by NIH grants: NS26528, GM088804, and GM080255.

References

Aceves-Pina EO, Quinn WG. Learning in normal and mutant *Drosophila* larvae. Science. 1979; 206:93–96. [PubMed: 17812455]

Asztalos Z, Arora N, Tully T. Olfactory jump reflex habituation in *Drosophila* and effects of classical conditioning mutations. J Neurogenet. 2007; 21:1–18. [PubMed: 17464794]

Baines RA. Postsynaptic protein kinase A reduces neuronal excitability in response to increased synaptic excitation in the *Drosophila* CNS. J Neurosci. 2003; 23:8664–8672. [PubMed: 14507965]

Balling A, Technau GM, Heisenberg M. Are the structural changes in adult Drosophila mushroom bodies memory traces? Studies on biochemical learning mutants. J Neurogenet. 1987; 4:65–73. [PubMed: 3598769]

Bellen HJ, Kiger JA Jr. Maternal effects of general and regional specificity on embryos of *Drosophila melanogaster* caused by *dunce* and *rutabaga* mutant combinations. Roux's Arch Dev Biol. 1988; 197:258–268.

Berke B, Wu CF. Regional calcium regulation within cultured *Drosophila* neurons: effects of altered cAMP metabolism by the learning mutations *dunce* and *rutabaga*. J Neurosci. 2002; 22:4437–4447. [PubMed: 12040051]

Bhattacharya A, Gu GG, Singh S. Modulation of dihydripyridine-sensitive calcium channels in *Drosophila* by a cAMP-mediated pathway. J Neurobiol. 1999; 39:491–500. [PubMed: 10380071]

Bradacs H, Cooper RL, Msghina M, Atwood HL. Differential physiology and morphology of phasic and tonic motor axons in a crayfish limb extensor muscle. J Exp Biol. 1997; 200:677–691. [PubMed: 9318419]

Brembs B, Plendl W. Double dissociation of PKC and AC manipulations on operant and classical learning in *Drosophila*. Curr Biol. 2008; 18:1168–1171. [PubMed: 18674907]

Budnik V, Zhong Y, Wu CF. Morphological plasticity of motor axons in Drosophila mutants with altered excitability. J Neurobiol. 1990; 10:3754–3768.

Byers D, Davis RL, Kiger JA Jr. Defect in cyclic AMP phosphodiesterase due to the *dunce* mutation of learning in *Drosophila melanogaster*. Nature. 1981; 289:79–81. [PubMed: 6256649]

Cann MJ, Levin LR. Restricted expression of a truncated adenylyl cyclase in the cephalic furrow of *Drosophila melanogaster*. Dev Genes Evol. 2000; 210:34–40. [PubMed: 10603085]

Chen CN, Denome S, Davis RL. Molecular analysis of cDNA clonse and the corresponding genomic coding sequences of the *Drosophila dunce*$^{+}$ gene, the structural gene for cAMP phosphodiesterase. Proc Natl Acad Sci USA. 1986; 83:9313–9317. [PubMed: 3025834]

Cheung US, Shayan AJ, Boulianne GL, Atwood HL. *Drosophila* larval neuromuscular junction's response to reduction of cAMP in the nervous system. J Neurobiol. 1999; 40:1–13. [PubMed: 10398067]

Cheung U, Atwood HL, Zucker RS. Presynaptric effectors contributing to cAMP-induced synaptic potentiation in *Drosophila*. J Neurobiol. 2006; 66:273–280. [PubMed: 16329127]

Corfas G, Dudai Y. Pharmacological evidence for the involvement of the cAMP cascade in sensory fatigue in *Drosophila*. J Comp Physiol A. 1990a; 167:437–440. [PubMed: 2172530]

Corfas G, Dudai Y. Adaptation and fatigue of a mechanosensory neuron in wild-type *Drosophila* and memory mutants. J Neurosci. 1990b; 10:491–499. [PubMed: 2154560]

Corfas G, Dudai Y. Morphology of a sensory neuron in *Drosophila* is abnormal in memory mutants and changes during aging. Proc Natl Acad Sci USA. 1991; 88:7252–7256. [PubMed: 1714597]

Das S, Sadanandappa MK, Dervan A, Larkin A, Lee JA, Sudhakaran IP, Priya R, Heidari R, Holohan EE, Pimentel A, Gandhi A, Ito K, Sanyal S, Wang JW, Rodrigues V, Ramaswami M. Plasticity of local GABAergic interneurons drives olfactory habituation. Proc Natl Acad Sci USA. 2011; 108:E646–E654. [PubMed: 21795607]

Davis RL. Olfactory memory formation in *Drosophila*: from molecular to systems neuroscience. Annu Rev Neurosci. 2005; 28:275–302. [PubMed: 16022597]

Davis RL, Kiger JA Jr. *dunce* mutants of *Drosophila melanogaster*: mutants defective in the cyclic AMP phosphodiesterase enzyme system. J Cell Biol. 1981; 90:101–107. [PubMed: 6265472]

Davis RL, Davidson N. The memory gene dunc^{+} encodes a remarkable set of RNAs with internal heterogeneity. Mol Cell Biol. 1986; 6:1464–1470. [PubMed: 2431279]

Davis GW, Schuster CM, Goodman CS. Genetic dissection of structural and functional components of synaptic plasticity. III. CREB is necessary for presynaptic functional plasticity. Neuron. 1996; 17:669–679. [PubMed: 8893024]

Day JP, Dow JAT, Houslay MD, Davies SA. Cyclic nucleotide phosphodiesterases in *Drosophila melanogaster*. Biochem J. 2005; 388:333–342. [PubMed: 15673286]

Del Castillo J, Katz B. Quantal components of the end-plate potential. J Physiol. 1954; 124:560–573. [PubMed: 13175199]

Delgado R, Davis R, Bono MR, Latorre R, Labarca P. Outward currents in *Drosophila* larval neurons: *dunce* lacks a maintained outward current component downregulated by cAMP. J Neurosci. 1998; 18:1399–1407. [PubMed: 9454849]

Devaud JM, Acebes A, Ferrus A. Odor exposure causes central adaptation and morphological changes in selected olfactory glomeruli in *Drosophila*. J Neurosci. 2001; 21:6274–6282. [PubMed: 11487650]

Devaud JM, Acebes A, Ramaswami M, Ferrus A. Structural and functional changes in the olfactory pathway of adult *Drosophila* take place at a critical age. J Neurobiol. 2003; 56:13–23. [PubMed: 12767029]

Devay P, Pinter M, Kiss I, Farago A, Friedrich P. Protein kinase C in larval brain of wild-type and dunce memory mutant *Drosophila*. J Neurogenet. 1989; 5:119–126. [PubMed: 2500506]

Dudai Y. Mutations affect storage and use of memory differentially in *Drosophila*. Proc Natl Acad Sci USA. 1983; 80:5445–5448. [PubMed: 16593363]

Dudai Y, Jan YN, Byers D, Quinn WG, Benzer S. *dunce*, a mutant of *Drosophila* deficient in learning. Proc Natl Acad Sci USA. 1976; 73:1684–1688. [PubMed: 818641]

Dudai Y, Uzzan A, Zvi S. Abnormal activity of adenylate cyclase in the *Drosophila* memory mutant rutabaga. Neurosci Lett. 1983; 42:207–212. [PubMed: 6420732]

Dudai Y, Zvi S. Adenylate cyclase in the *Drosophila* memory mutant rutabaga displays an altered Ca^{2+} sensitivity. Neurosci Lett. 1984; 47:119–124. [PubMed: 6462535]

Duerr JS, Quinn WG. Three *Drosophila* mutations that block associative learning also affect habituation and sensitization. Proc Natl Acad Sci USA. 1982; 79:3646–3650. [PubMed: 6808513]

Engel JE, Wu CF. Altered habituation of an identified escape circuit in *Drosophila* memory mutants. J Neurosci. 1996; 16:3486–3499. [PubMed: 8627381]

Engel JE, Xie XJ, Sokolowski MB, Wu CF. A cGMP-dependent protein kinase gene, foraging, modifies habituation-like response decrement of the giant fiber escape circuit in *Drosophila*. Learn Mem. 2000; 7:341–352. [PubMed: 11040266]

Engel JE, Wu CF. Neurogenetic approaches to habituation and dishabituation in *Drosophila*. Neurobiol Learn Mem. 2009; 92:166–175. [PubMed: 18765288]

Fatt P, Katz B. Spontaneous subthreshold activity at motor nerve endings. J Physiol. 1952; 117:109–128. [PubMed: 14946732]

Feany MB. Rescue of the learning defect in dunce, a *Drosophila* learning mutant, by an allele of rutabaga, a second learning mutant. Proc Natl Acad Sci USA. 1990; 87:2795–2799. [PubMed: 2157213]

Feng Y, Ueda A, Wu CF. A modified minimal hemolymph-like solution, HL3.1, for physiological recordings at the neuromuscular junctions of normal and mutant *Drosophila* larvae. J Neurogenet. 2004; 18:377–402. [PubMed: 15763995]

Featherstone DE, Rushton EM, Hilderbrand-Chae M, Phillips AM, Jackson FR, Broadie K. Presynaptic glutamic acid decarboxylase is required for induction of the postsynaptic receptor field at a glutamatergic synapse. Neuron. 2000; 27:71–84. [PubMed: 10939332]

Folkers E. Visual learning and memory of *Drosophila melanogaster* wild type C-S and the mutants *dunce*, *amnesiac*, *turnip* and *rutabaga*. J Insect Physiol. 1982; 28:535–539.

Gailey DA, Jackson FR, Siegel RW. Conditioning mutations in *Drosophila melanogaster* affect an experience-dependent behavioral modification in courting males. Genetics. 1984; 106:613–623. [PubMed: 17246201]

Ganetzky B, Wu CF. Drosophila mutants with opposing effects on nerve excitability: genetic and spatial interactions in repetitive firing. J Neurophysiol. 1982a; 47:501–514. [PubMed: 6279790]

Ganetzky B, Wu CF. Indirect suppression involving behavioral mutants with altered nerve excitability in *Drosophila melanogaster*. Genetics. 1982b; 100:597–614. [PubMed: 17246073]

Gong ZF, Xia SZ, Liu L, Feng CH, Guo AK. Operant visual learning and memory in *Drosophila* mutants *dunce*, *amnesiac* and *radish*. J Insect Physiol. 1998; 44:1149–1158. [PubMed: 12770314]

Griffith LC, Wang J, Zhong Y, Wu CF, Greenspan RJ. Calcium/calmodulin-dependent protein kinase II and potassium channel subunit Eag similarly affect plasticity in *Drosophila*. Proc Natl Acad Sci USA. 1994; 91:10044–10048. [PubMed: 7937834]

Griffith LC, Ejima A. Courtship learning in *Drosophila melanogaster*: diverse plasticity of a reproductive behavior. Learn Mem. 2009; 16:743–750. [PubMed: 19926779]

Han PL, Levin LR, Reed RR, Davis RL. Preferential expression of the Drosophila *rutabaga* gene in mushroom bodies, neural centers for learning in insects. Neuron. 1992; 9:619–627. [PubMed: 1382471]

Iourgenko V, Levin LR. A calcium-inhibited *Drosophila* adenylyl cyclase. Biochim Biophys Acta. 2000; 1495:125–139. [PubMed: 10656970]

Iourgenko V, Kilot B, Cann MJ, Levin LR. Cloning and characterization of Drosophila adenylyl cyclase homologous to mammalian type IX. Febs Lett. 1997; 413:104–108. [PubMed: 9287125]

Johannessen M, Moens U. Multiple phosphorylation of the cAMP response element-binding protein (CREB) by a diversity of protein kinases. Front Biosci. 2007; 12:1814–1832. [PubMed: 17127423]

Kauvar LM. Defective cyclic adenosine 3′:5′-monophosphate phosphodiesterase in the *Drosophila* memory mutant *dunce*. J Neurosci. 1982; 2:1347–1358. [PubMed: 6288893]

Kim YT, Wu CF. Reduced growth cone motility in cultured neurons from *Drosophila* memory mutants with a defective cAMP cascade. J Neurosci. 1996; 16:5593–5602. [PubMed: 8795615]

Kurdyak P, Atwood HL, Stewart BA, Wu CF. Differential physiology and morphology of motor axons to ventral longitudinal muscles in larval Drosophila. J Comp Neurol. 1994; 350:463–472. [PubMed: 7884051]

Kuromi H, Kidokoro Y. Tetanic stimulation recruits vesicles from reserve pool via a cAMP-mediated process in *Drosophila* synapses. Neuron. 2000; 27:133–143. [PubMed: 10939337]

Larkin A, Karak S, Priya R, Das A, Ayyub C, Ito K, Rodrigues V, Ramaswami M. Central synaptic mechanisms underlie short-term olfactory habituation in *Drosophila* larvae. Learn Mem. 2010; 17:645–653. [PubMed: 21106688]

Lee J, Ueda A, Wu CF. Pre- and post-synaptic mechanisms of synaptic strength homeostasis revealed by *slowpoke* and *Shaker* K^+ channel mutations in *Drosophila*. Neurosci. 2008; 154:1283–1296.

Levin LR, Han PL, Hwang PM, Feinstein PG, Davis RL, Reed RR. The Drosophila learning and memory gene *rutabaga* encodes a Ca^{2+}/calmodulin-responsive adenylyl cyclase. Cell. 1992; 68:479–489. [PubMed: 1739965]

Liu G, Seiler H, Wen A, Zars T, Ito K, Wolf R, Heisenberg M, Liu L. Distinct memory traces for two visual features in the *Drosophila* brain. Nature. 2006; 439:551–556. [PubMed: 16452971]

Livingstone MS, Sziber PP, Quinn WG. Loss of calcium/calmodulin responsiveness in adenylate cyclase of *rutabaga*, a Drosophila learning mutant. Cell. 1984; 37:205–215. [PubMed: 6327051]

Mery F, Belay AT, So AKC, Sokolowski MB, Kawecki TJ. Natural polymorphism affecting learning and memory in *Drosophila*. Proc Natl Acad Sci USA. 2007; 104:13051–13055. [PubMed: 17640898]

Mohler D, Carroll A. Sex-linked female-sterile mutations in the Iowa collection. DIS. 1984; 60:236–241.

Moore MS, DeZazzo J, Luk AY, Tully T, Singh CM, Heberlein U. Ethanol Intoxication in *Drosophila*: genetic and pharmacological evidence for regulation by the cAMP signaling pathway. Cell. 1998; 93:997–1007. [PubMed: 9635429]

Nighorn A, Healy MJ, Davis RL. The cyclic AMP phosphodiesterase encoded by the Drosophila *dunce* gene is concentrated in the mushroom body neuropil. Neuron. 1991; 6:455–467. [PubMed: 1848082]

Peng IF, Berke BA, Zhu Y, Lee WH, Chen W, Wu CF. Temperature-dependent developmental plasticity of *Drosophila* neurons: cell-autonomous roles of membrane excitability, Ca^{2+} influx, and cAMP signaling. J Neurosci. 2007; 27:12611–12622. [PubMed: 18003840]

Qiu Y, Chen CN, Malone T, Richter L, Beckendorf SK, Davis RL. Characterization of the memory gene dunce of *Drosophila melanogaster*. J Mol Biol. 1991; 222:553–565. [PubMed: 1660926]

Renger JJ, Yao W-D, Sokolowski MB, Wu C-F. Neuronal polymorphism among natural alleles of a cGMP-dependent kinase gene, *foraging*,in *Drosophila*. J Neurosci. 1999; 19:RC28. [PubMed: 10493773]

Renger JJ, Ueda A, Atwood HL, Govind CK, Wu CF. Role of cAMP cascade in synaptic stability and plasticity: Ultrastructural and physiological analysis of individual synaptic boutons in *Drosophila* memory mutants. J Neurosci. 2000; 20:3980–3992. [PubMed: 10818133]

Salz HK, Davis RL, Kiger JA Jr. Genetic analysis of chromomere 3D4 in *Drosophila melanogaster*: the *dunce* and *sperm-amotile* gene. Genetics. 1982; 100:587–596. [PubMed: 17246072]

Schuster CM, Davis GW, Fetter RD, Goodman CS. Genetic dissection of structudal and functional components of synaptic plasticity. II. Fasciclin II controls presynaptic structural plasticity. Neuron. 1996; 17:655–667. [PubMed: 8893023]

Sigrist SJ, Thiel PR, Reiff DF, Lachance PED, Lasko P, Schuster GM. Postsynaptic translation affects the efficacy and morphology of neuromuscular junctions. Nature. 2000; 405:1062–1065. [PubMed: 10890448]

Song HJ, Ming GL, Poo M-m. cAMP-induced switching in turning direction of nerve growth cones. Nature. 1997; 388:275–279. [PubMed: 9230436]

Suzuki K, Grinnell AD, Kidokoro Y. Hypertonicity-induced transmitter release at Drosophila neuromuscular junctions is partly mediated by integrins and cAMP/protein kinase A. J Physiol. 2002; 538:103–119. [PubMed: 11773320]

Technau GM. Fiber number in the mushroom bodies of adult Drosophila melanogaster depends on age, sex and experience. J Neurogenet. 1984; 1:113–126. [PubMed: 6085635]

Tempel BL, Bonini N, Dawson DR, Quinn WG. Reward learning in normal and mutant *Drosophila*. Proc Natl Acad Sci USA. 1983; 80:1482–1486. [PubMed: 6572401]

Tully T, Quinn WG. Classical conditioning and retention in normal and mutant *Drosophila melanogaster*. J Comp Physiol A. 1985; 157:263–277. [PubMed: 3939242]

Tully T, Gold D. Differential effects of dunce mutations on associative learning and memory in Drosophila. J Neurogenet. 1993; 9:55–71. [PubMed: 8295077]

Ueda A, Wu CF. Role of rut adenylyl cyclase in the ensemble regulation of presynaptic terminal excitability: reduced synaptic strength and precision in a Drosophila memory mutant. J Neurogenet. 2009; 23:185–199. [PubMed: 19101836]

Wustmann G, Rein K, Wolf R, Heisenberg M. A new paradigm for operant conditioning of *Drosophila melanogaster*. J Comp Physiol A. 1996; 179:429–436. [PubMed: 8785009]

Yao WD, Wu CF. Distinct roles of CaMKII and PKA in regulation of firing patterns and K^+ currents in *Drosophila* neurons. J Neurophysiol. 2001; 85:1384–1394. [PubMed: 11287463]

Yao WD, Rusch J, Poo M-m, Wu CF. Spontaneous acetylcholine secretion from developing growth cones of *Drosophila* central neurons in culture: effects of cAMP-pathway mutations. J Neurosci. 2000; 20:2626–2637. [PubMed: 10729343]

Zars T, Wolf R, Davis R, Heisenberg M. Tissue-specific expression of a type I adenylyl cyclase rescues the *rutabaga* mutant memory defect: in search of the engram. Learn Mem. 2000; 7:18–31. [PubMed: 10706599]

Zhao ML, Wu CF. Alterations in frequency coding and activity dependence of excitability in cultured neurons of *Drosophila* memory mutants. J Neurosci. 1997; 17:2187–2199. [PubMed: 9045743]

Zhong Y, Wu CF. Altered synaptic plasticity in *Drosophila* memory mutants with a defective cyclic AMP cascade. Science. 1991; 251:198–201. [PubMed: 1670967]

Zhong Y, Budnik V, Wu CF. Synaptic plasticity in *Drosophila* memory and hyperexcitable mutants: role of cAMP cascade. J Neurosci. 1992; 12:644–651. [PubMed: 1371316]

Zhong Y, Wu CF. Differential modulation of potassium currents by cAMP and its long-term and short-term effects: *dunce* and *rutabaga* mutants of *Drosophila*. J Neurogenet. 1993; 9:15–27. [PubMed: 8295075]

Zhong Y, Wu CF. Neuronal activity and adenylyl cyclase in environment-dependent plasticity of axonal outgrowth in *Drosophila*. J Neurosci. 2004; 24:1439–1445. [PubMed: 14960616]

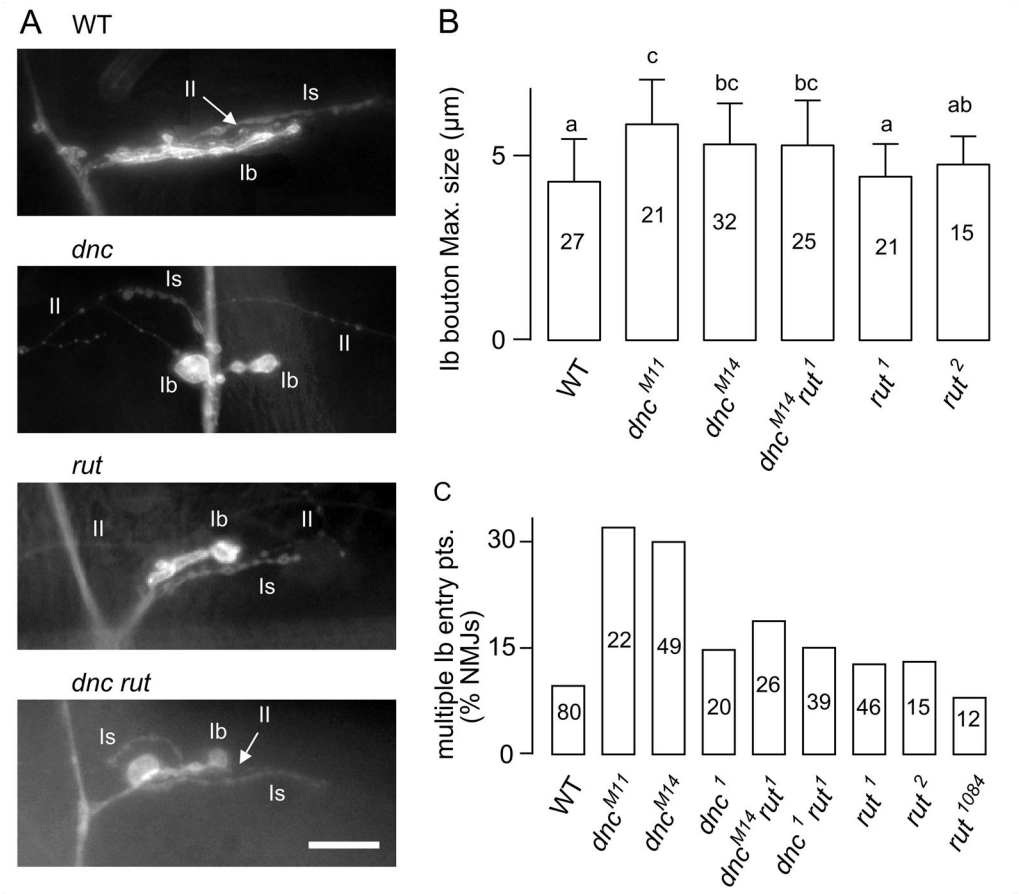

Figure 1.

Neuromuscular junction morphological defects in *dnc*, *rut*, and *dnc rut* larvae. (A) Anti-HRP antibody immunostaining in third instar larvae. Note that *dnc* and *dnc rut* displayed strikingly large type Ib boutons. Furthermore, the Ib and Is branches were dissociated in their projection in *dnc*. Typically Ib and Is branches run in parallel as shown in WT, *rut*, and *dnc rut*. (B) Boutons of larger sizes were more common in *dnc* larvae, as demonstrated by the diameter of largest bouton within individual NMJs. This phenotype was not rescued in the *dnc rut* double mutant. (C) Percentage of NMJs with multiple nerve entry points of Ib branch. Such abnormal ectopic entry was significantly increased in dnc^{M11} and dnc^{M14}, but not in dnc^{1}. This was not affected by *rut* and was partially rescued in the *dnc rut* double mutant. Groups of a, b, and c in (A) indicate significant differences between the group ($p < 0.05$; one-way ANOVA). Error bars indicate SD.

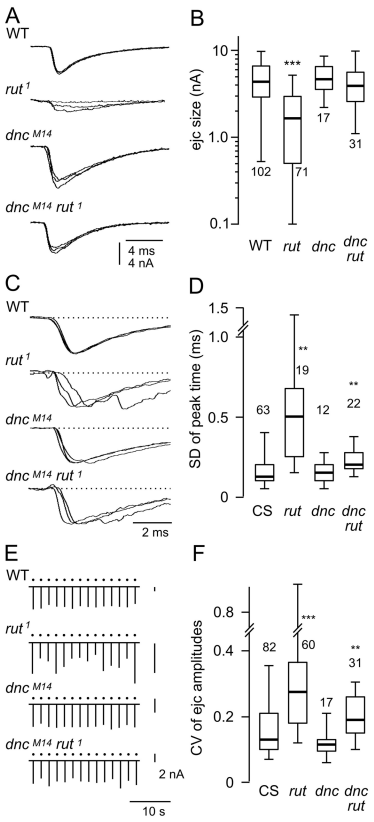

Figure 2.

Amplitude and temporal precision of transmitter release. Focal excitatory junctional current (ejc) recordings were performed in HL3 saline containing a physiological Ca^{2+} concentration, 1.5 mM. (A) Typical ejc traces from WT (CS), *rut*^{1}, *dnc*^{M14}, and *dnc*^{M14} *rut*^{1}. Three consecutive ejcs are overlayed for each genotype. Note that ejcs in *rut*^{1} is significantly smaller and more variable than WT. (B) The amplitude of ejcs were significantly smaller in *rut*, but not in *dnc* or *dnc rut*. Note the log scale. (C, D) Variability of the time course of transmitter release. Three consecutive ejcs are normalized and overlaid to enhance the visibility of time course variation (C). Ejc time course variation as indicated by the SD of time to peak (D). Ejc peak time was highly variable in *rut*, but not in *dnc*. The defect was not totally rescued in *dnc rut* double mutants. (E, F) Transmitter release variability as indicated by ejc fluctuation during repeated nerve stimulation. (E) Consecutive ejcs displayed for each genotype over 30 seconds of repetitive stimulation (0.5 Hz, dots). Note different scale bars for different genotypes. (F) CV of ejc amplitudes was significantly increased in *rut*, but not in *dnc*. The *rut* defect was only partially rescued in *dnc rut*. For each box plot, the number of NMJs examined is indicated. ***, **, and * indicates $p < 0.001$, 0.01, and 0.05, respectively (rank-test with Bonferroni correction for multiple comparisons). Genotypes used include *rut*^{1}, *dnc*^{M14}, *dnc*^{M14} *rut*^{1}, and *dnc*^{1} *rut*^{1}.

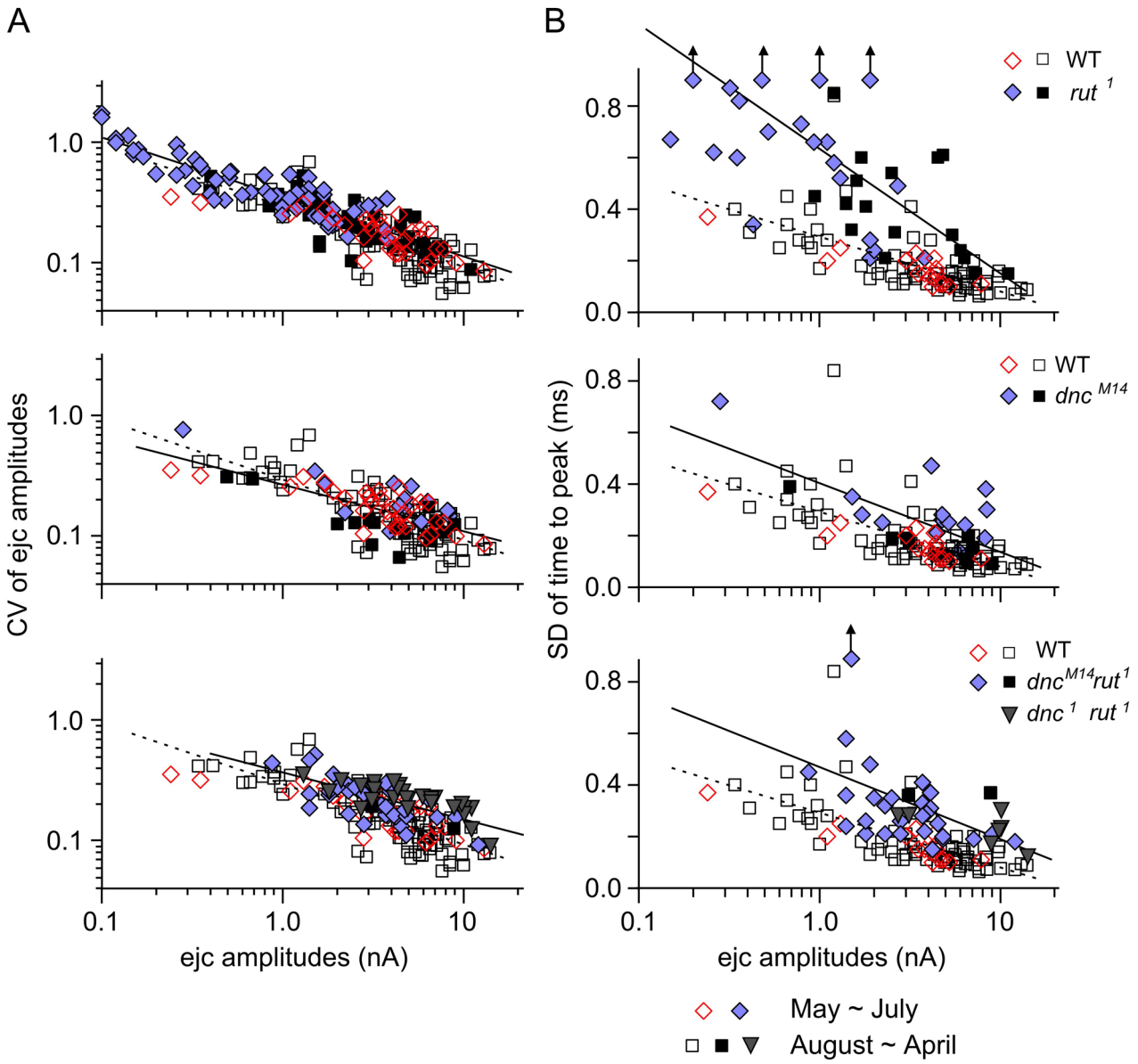

Figure 3.

Altered release properties in *rut*, *dnc*, and *dnc rut*. (A) CV of focal ejc size is displayed as a function of averaged ejc amplitude from individual recording sites. In each panel, *rut*, *dnc*, and *dnc rut* data are plotted against WT data. Note that the slope of the regression lines for both WT and mutants was about 1/2, as expected from the quantal nature of transmitter release (see text). Therefore the magnitude of amplitude fluctuation in Fig. 2 could be predicted by the amount of release in different genotypes. (B) SD of time to peak plotted against ejc amplitude. Variability in peaking time was larger in *rut*, *dnc*, and *dnc rut* compared to WT over the range of focal ejc sizes, indicating loose temporal regulation of vesicle release. The deviation from WT was greatest in *rut*, which was partially corrected in *dnc rut* double mutants. Regression lines for both WT (dotted) and mutants (solid) are shown in each panel for comparison. Different symbols indicate data from different periods of the year (See Fig. 4). Data points represents individual recording sites along different motor terminal branches. The number of branches in A and B is 82 and 63 (WT CS), 60 and

19 (*rut*^{1}), 17 and 12 (*dnc*^{M14}), 19 and 17 (*dnc*^{M14} *rut*^{1}), and 12 and 5 (*dnc*^{1} *rut*^{1}), respectively. The number of recording sites in A and B is 116 and 86 (WT CS), 105 and 38 (*rut*^{1}), 31 and 25 (*dnc*^{M14}), 39 and 31 (*dnc*^{M14} *rut*^{1}), and 27 and 7 (*dnc*^{1} *rut*^{1}), respectively.

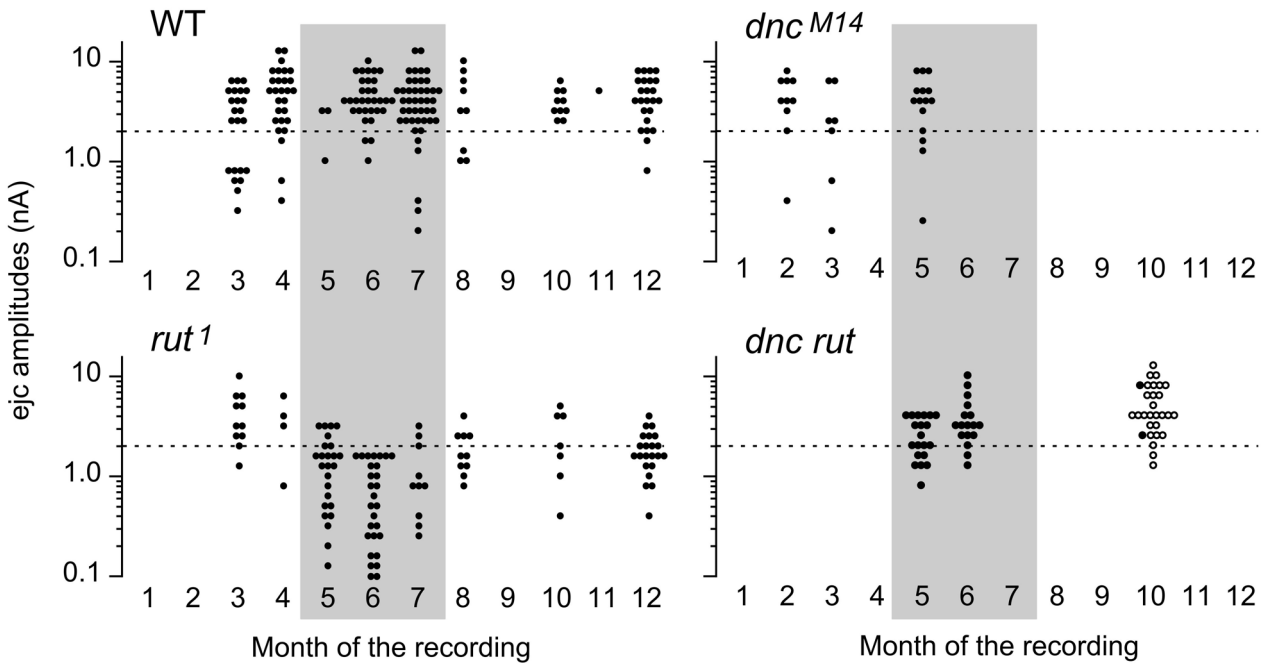

Figure 4.

Seasonal variation of focal ejc amplitude in *rut*. Note that ejcs from the majority of *rut* boutons were below 2 nA (dotted line) during the months of May, June, and July (shaded period) whereas ejcs collected outside of this period was substantially larger. In contrast, ejcs from WT, *dnc*, and *dnc rut* did not show such a seasonal effect. During these months, room temperature were higher, approaching 30°C. Ejcs were collected from 6/1998 – 8/2001 for WT, from 5/1998 to 10/2001 for *rut*, from 2/2000 – 5/2000 for *dnc*, from 5/1999 – 10/2001 for dnc^{M14} rut^{1}, in 10/2001 for dnc^{1} rut^{1}. For double mutants, ●: dnc^{M14} rut^{1}, ○: dnc^{1} rut^{1}. Data points represents individual recording sites along different motor terminal branches. The number of branches is 102 (WT CS), 68 (rut^{1}), 17 (dnc^{M14}), 19 (dnc^{M14} rut^{1}), and 12 (dnc^{1} rut^{1}), respectively. The number of recording sites is 175 (WT CS), 122 (rut^{1}), 34 (dnc^{M14}), 39 (dnc^{M14} rut^{1}), and 27 (dnc^{1} rut^{1}), respectively.

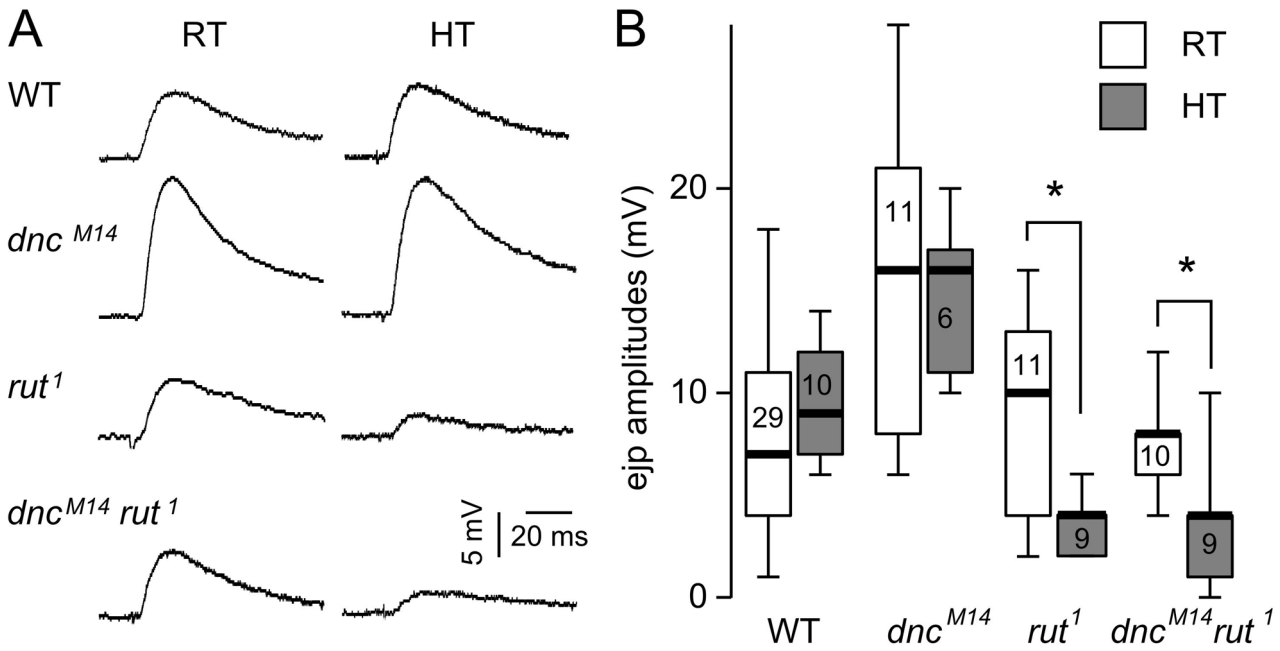

Figure 5.

Effects of rearing temperature on ejp size. (A) Representative ejp traces from larvae reared at RT (22–24 °C) or at high temperature (HT, 29–30 °C). Ejps were recorded from muscles 6 and 7. Ejps in *rut*^{1} showed significantly reduced amplitude when larvae were grown at HT but those in WT and *dnc* larvae did not appear to be affected by rearing temperature. This abnormal temperature response of *rut*^{1} was not rescued in *dnc*^{M14} *rut*^{1} double mutants. (B) Box plot summarizing the statistics of rearing temperature effects for different genotypes. The number indicates the muscle sample size. * indicates $p < 0.05$ (rank-test with Bonferroni correction for multiple comparisons).

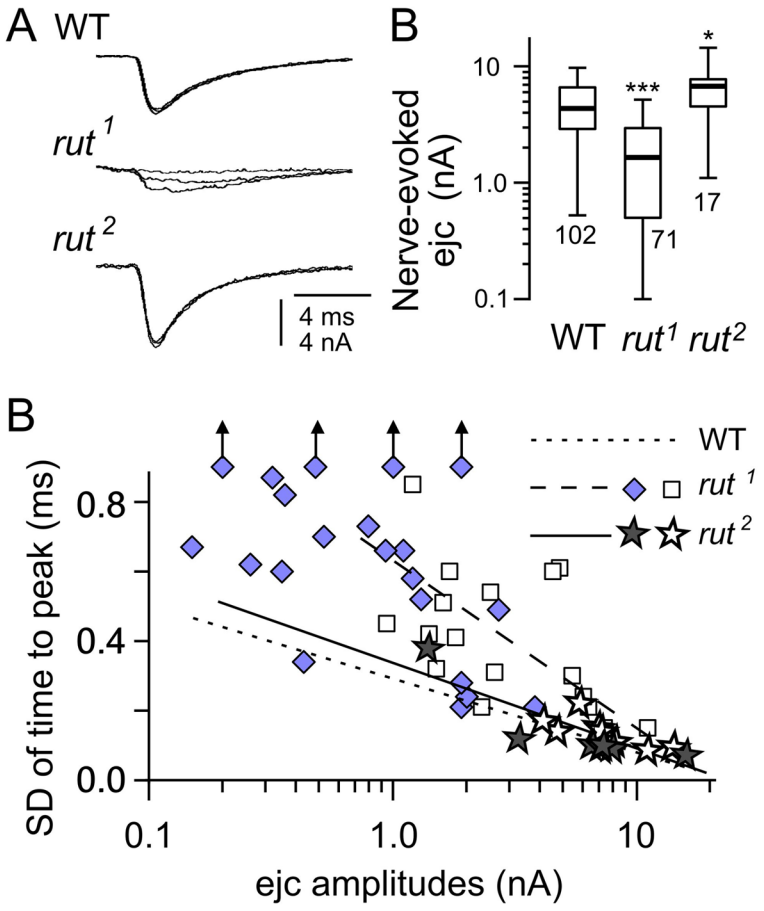

Figure 6.

Comparison of neurotransmission in *rut*[1] and *rut*[2]. (A) Moderately increased in ejc amplitude in *rut*[2] as opposed to severely depressed transmission in *rut*[1]. *** and * indicates $p < 0.001$ and 0.05, respectively (rank-test with Bonferroni correction for multiple comparison). (B) Severity of the defect in release timing was much less in *rut*[2] compared to *rut*[1]. Regression lines are shown for WT, *rut*[1], and *rut*[2]. Filled symbols: collected on May - July. Open symbols: collected on August - April. Data for *rut*[2] were collected from 3/2000 to 6/2000. Data for *rut*[1] are shown but WT data are omitted for clarity (cf. Fig. 3).

Table 1

Neural and behavioural phenotypes of *rut, dnc,* and *dnc rut* mutants

Phenotype	*rut*	*dnc*	*dnc rut*	Comments (order of severity, etc)	References
I. Neuronal development					
a. Cultured neurons					
Growth cone (GC) motility	↓	↓	Restored * to normal	db-cAMP rescues *rut.* Forskolin mimics *dnc.* $dnc^{M11} = dnc^{M14} = dnc^{1} <$ WT $dnc^{M14}rut^{1} = dnc^{1}\ rut^{1} =$ WT	Kim & Wu (1996)
Spontaneous transmitter release from GC	ND	Decreased but prolonged release	ND	db-cAMP mimic *dnc.* Similar results observed in PKA regulatory subunit mutant *PKA-RI.*	Yao et al. (2000)
Hyperexcitability-induced increase in GC size	↓	ND	ND	*Sh* mutations- or4-aminopyrine-induced hyperexcitability. $rut^{1} = rut^{2}$ < WT	Peng et al., (2007)
HT- or hyperexcitability-increase in neurite branching	↓	ND	ND	"	"
b. Larval NMJ					
synaptic protein expression	ND	Altered	ND	elF4E ↑; FasII ↓; dGluRIIA ↑ in *dnc*	Schuster et al. (1996); Sigrist et al. (2000)
Bouton size	Normal	↑	↑	$dnc^{M11} = dnc^{M14} = dnc^{M14}rut^{1} >$ WT	This paper
Motor terminal growth	Normal	↑	Restored * to normal	$dnc^{M14} = dnc^{M11/1} = dnc^{1} >$ WT $dnc^{M14}\ rut^{2} > dnc^{M14}rut^{1} =$ WT	Zhong et al. (1992)
				FasII and CREB involved.	Schuster et al. (1996)
				Decreased by expression of UAS-dnc^{+} in motorneurons.	Cheung et al. (1999)
HT- or hyperexcitability-induced motor terminal growth	↓	↑	ND	*eag* and *Sh* mutation-induced hyperexcitability $rut^{1} = rut^{2080} <$ WT $< dnc^{M11}/dnc^{1} = dnc^{1}$	Zhong et al. (1992); Zhong & Wu (2004)
Motor terminal projection pattern	Normal	Ib/Is branches dissociation	Partial restoration * toward normal	$dnc^{M14} = dnc^{M11} = dnc^{1}$ $> dnc^{M14}\ rut^{1} = dnc^{1}\ rut^{1} >$ WT	This paper
No. motor terminal entry points	Normal	↑	Partial restoration * toward normal	Presence of ectopic nerve entry to muscle fibers $dnc^{M14} = dnc^{M11}$ $> dnc^{M14}rut^{1} = dnc^{1}\ rut^{1} = dnc^{1} =$ WT	"
c. Adult mushroom bodies					
No. axons in peduncles (young)	Normal	↑	ND	No. axons increases during maturation. $dnc^{M11} = dnc^{1} >$ WT	Technau (1984); Balling et al. (1987)
(mature)	↓	Normal	ND		
Lobe size	Normal	↑	ND		Peng et al., (2007)

Phenotype	*rut*	*dnc*	*dnc rut*	Comments (order of severity, etc)	References
d. Adult mechanosensory cell					
No. varicosities and branches	↑	↑	ND	HRP backfill	Corfas & Dudai (1991)
II. Ionic currents and membrane excitability					
a. Cultured neurons					
Regularity in firing pattern	↓	↓	↓	Whole-cell action potential recording. dnc^{M11} rut^{2} was used.	Zhao & Wu (1997)
				Consistent effect observed in the PKA catalytic subunit mutant *DCO*.	Yao & Wu (2001)
K^+ current	↓	↓ Sustained current	↓	Whole-cell recording of both sustained and transient currents. dnc^{M11} rut^{2} was used.	Zhao & Wu (1997); Delgado et al. (1998)
b. Larval muscles					
K^+ current					
i) IA & IK	Normal	↑	ND	db-cAMP in WT increases IA but not IK. $dnc^{1} = dnc^{2} = dnc^{1}/+ = dnc^{2}/+ >$ WT	Zhong & Wu (1993)
ii) ICS	↓	ND	ND	db-cAMP in *rut* does not rescue ICS.	“
Ca^{2+} current	↓	↑	ND	Forskolin or 8Br-cAMP mimics *dnc*. H89, a PKA Blocker, mimics *rut*. $dnc^{2} \geqq dnc^{1} >$ WT $> rut^{1} \geqq rut^{2}$	Bhattacharya et al. (1999)
c. Larval central neurons					
Motor neuron somata					
i) Na^+ current	ND	↓	ND	Sp-cAMPS mimics *dnc*.	Baines (2003)
ii) Firing frequency	ND	↓	ND	“ $dnc^{2} = dnc^{1} <$ WT	“
III. Enzyme activity and Ca^{2+} dynamics					
a. Enzyme activity					
Adenylyl cyclase	↓	Normal	↓	$rut^{1} < rut^{2} = rut^{3} <$ WT	Dudai et al. (1983); Dudai & Zvi (1984); Livingstone et al. (1984); Feany (1990)
Phosphodiesterase	Normal	↓	↓	$dnc^{M11} = dnc^{M14} < dnc^{1} <$ WT	Davis & Kiger (1981); Byers et al. (1981)
b. Ca^{2+}dynamics in cultured neurons					
Amplitudes in GC	↓	↓	ND	High K^+ -induced Ca^{2+} influx, detected by fura-2 AM	Berke & Wu (2002)
Duration at soma	↑	↑	ND	“	“

Phenotype	*rut*	*dnc*	*dnc rut*	Comments (order of severity, etc)	References
IV. Synaptic structure and function at larval NMJs					
a. Evoked transmitter release					
Whole-cell ejp amplitude					
i) Larvae reared at RT	Normal	Normal/↑	Nearly normal	$dnc^{M14} > dnc^{1}$ = WT $dnc^{M14}rut^{1}$ nearly WT (see text).	This paper
				Decreased by expression of UAS-dnc^{+} in motor neurons. Increased by forskolin.	Cheung et al. (1999); Cheung et al. (2006)
ii) Larvae reared at HT	↓	↑	↓	dnc^{1} not examined.	This paper
Whole-cell ejc amplitude					
i) Amplitude	Normal	↑	ND	$dnc^{M11} = dnc^{M14} >$ WT	Zhong & Wu (1991)
ii) Activity-dependent facilitation & potentiation	↓	↓	ND	$dnc^{M11} = dnc^{M14} < dnc^{1} <$ WT db-cAMP partially mimics *dnc* and partially rescues *rut.*	"
Focal ejcs from boutons					
I) Amplitude	↓	Normal	Nearly normal	$rut^{1} = rut^{1084} <$ WT = $dnc^{M11} = dnc^{2}$ Slight reduction by db-cAMP and Rp-cAMPS in WT. *dnc rut* nearly normal (see text).	Renger et al. (2000); Ueda & Wu (2009); This paper
ii) Synchronicity of release	↓	↓	↓	Not mimiced by db-cAMP or Rp-cAMPS in WT.	Renger et al. (2000)
b. Synaptic vesicles					
Hypertonicity-induced discharge	Normal	↑	ND	High-sucrose evoked ejcs in 1st instar larvae. Forskolin mimics *dnc*	Suzuki & Kidokoro (2002)
High-frequency-stimulation-induced translocation from reserve pool to Exo/Endo cycling pool	↓	↑	ND	Visualized with FM1–43 Forskolin mimics *dnc.* Rp-cAMPS mimics *rut.*	Kuromi & Kidokoro (2000)
c. Synaptic ultrastructure					
Docked vesicle/synapse	↓	↑	ND		Renger et al. (2000)
Synapse size	↑	Normal	ND		"
No. Synapses	↓	Normal	ND		"
V. Conditioned behaviors and related physiology					
a. Non-associative conditioning					
Fatigue					
Decrease in mechanosensory cell firing	Slow	Fast	ND	Forskolin mimic *dnc* and H7 (PKA inhibitor) mimic *rut.*	Corfas & Dudai (1990a, b)

Phenotype	*rut*	*dnc*	*dnc rut*	Comments (order of severity, etc)	References
Adaptation to odor exposure					
Adaptation of olfactory response and reduction of olfactory glomeruli volume	↓	↓	ND		Devaud et al. (2001, 2003)
Habituation rate					
i) Giant fiber pathway escape reflex	↓	↑	↑↑		Engel & Wu (1996)
ii) Olfactory avoidance and jump response	↓	↓	ND	$dnc^{M14} = dnc^{1} <$ WT	Asztalos et al. (2007) Das et al. (2011)
iii) Proboscis extension reflex	↓	↓	ND	$dnc^{1} = dnc^{2} <$ WT	Duerr & Quinn (1982)
iv) Larval chemotaxis	↓	ND	ND		Larkin et al. (2010)
b. Associative learning					
Classical conditioning paradigm					
i) Color & shaking of adult flies	↓	↓	ND		Folkers (1982)
ii) Odor & electrical shock in adults	↓	↓	↓	$dnc^{M11}\ rut^{1} < dnc^{M14} = dnc^{1} = rut^{1} \leqq dnc^{2} <$ WT	Dudai et al., (1976); Dudai (1983); Tully & Quinn (1985); Tully & Gold (1993)
				$dnc^{M14}rut^{1} = dnc^{M14}rut^{3} = dnc^{M14} = rut^{1} < rut^{2} = dnc^{M14}rut^{2} < rut^{3} = rut^{1/3} = rut^{1/2} =$ WT	Feany (1990)
iii) Odor & electrical shock in larvae	ND	↓	ND		Aceves-Pina & Quinn (1979)
iv) Odor & sucrose reward in adults	↓	↓	ND		Tempel et al. (1983)
v) Courtship conditioning	↓	↓	ND		Gailey et al. (1984)
Operant conditioning paradigm					
I) Flight simulator	↓	↓	ND	Visual cue-associated with heat punishment in flight simulator.	Gong et al. (1998); Liu et al. (2006) Brembs & Plendl (2008)
ii) Heat box	↓	↓	ND	Spatial cue-associated with heat punishment	Wustmann et al. (1996); Zars et al. (2000)
c. Ethanol tolerance	↓	Normal	ND		Moore et al. (1998)

↑, ↓, Normal: greater than, less than, or similar to WT;

*: successful counter balancing rescue in *dnc rut;* ND: not determined

CREB: cAMP response element binding protein; dGluRIIA: *Drosophila* glutamate receptor subunit IIA; elF4E: eukaryotic translation initiation factor 4E; FasII: Fasciclin II; forskolin: activator of adenylyl cyclase; GC: growth cone; HT: High temperature (29~30 °C); NMJ: neuromuscular junction;